Engineering Innovations
ISSN: 2813-1002, Vol. 6, pp 1-22
doi:10.4028/p-gdl41l

Submitted: 2023-02-05
Revised: 2023-02-25
Accepted: 2023-03-23
Online: 2023-06-21

The Impact of Gas-Liquid Dispersed Flow on Heat Exchanger Performance with Improvement Using CuO Nanofluid

Mustafa M. Hathal[1,2,a*], Basim O. Hasan[2,4,b], Hasan Sh. Majdi[2,c]

[1]The Industrial Development and Regulatory Directorate/ The Ministry of Industry and Minerals/ Baghdad- Iraq.

[2]The Scientific Society for Energy Studies and Research/ Baghdad- Iraq.

[3]Chemical Engineering and Petroleum Industry Department/ Al-Mustaqbal University College/ Hilla- Iraq.

[4]Chemical Engineering Department/ Al-Nahrain University/ Baghdad- Iraq.

*Corresponding Email: [a]mus.mhathal@gmail.com, [b]basimohasan13@gmail.com, [c]hasanshker1@gmail.com

Keywords: heat transfer, dispersion, air bubbles, copper oxide nanofluid

Abstract. Both the air-water dispersion coefficient and the air-nanofluid (CuO) dispersion coefficient were studied and measured in a double-pipe heat exchanger. Pumping air into a tank fitted with a Rushton turbulent impeller resulted in gas-liquid dispersion. In order to test the effects of varying operating conditions on the air-water and air-nanofluid dispersions, they were heated and pumped into the tube of a double-pipe heat exchanger. Reynolds numbers of Re_c= 4750-13100 on the shell side and Re_h=19900-64000 on the tube side were used to get the total heat transfer coefficient (U_o). The dispersion in the hot fluid tank was achieved by combining the two-phase fluids using a Rushton turbine impeller. It was discovered that the conscious phase saw a significant drop in the heat transfer coefficient when the air bubbles dissipated. Because the impeller's agitation speed affects the rate at which air bubbles are broken, the heat transfer coefficient in the case of dispersion rises as Reh and Rec rise. For all examined parameter values, CuO nanofluid showed significant heat transfer improvement. The heat transfer rate of gas-liquid dispersion was increased by nanofluid by as much as 135.5% compared to gas-liquid dispersion..

1. Introduction

Multiphase flows, which involve dispersions of gas-liquid, liquid-liquid, and solid-liquid, are commonly observed in numerous industrial applications. Dispersants are utilized in a variety of industrial processes, such as petroleum refining, bio-chemical reactor operation, mixing procedures, food production, metalworking, and numerous other applications. The rate of heat transfer during heat treatment processes is influenced by the presence of dispersants with varying concentrations and properties in the process or working fluids. Heat exchangers find extensive usage in diverse industrial sectors such as oil and gas industries, thermal power plants, refrigeration systems, cooling of electronics, air conditioning, and automobiles, among others [1]. They are employed for cooling, heating, or phase changing purposes. Enhancing the heat transfer properties facilitates the conservation of energy, reduction of expenses, and enhancement of product excellence [2]. The phenomenon of gas-liquid dispersion is a common occurrence in a variety of industrial settings, characterized by the presence of two distinct phases. Gas-liquid dispersion cases find common applications in various processes such as petroleum processing from wells, air-liquid mixing and separation, fermentation, bubble columns, solar collectors, and nuclear reactors [3]. Gas-liquid dispersion is a phenomenon that frequently transpires in geothermal wells. This can be attributed to the pressure gradient within refinery distillation towers or the presence of a non-boiling gas phase that disperses within the liquid phase, such as oil-gas in pore wells [4].Research pertaining to the impact of multiphase flows on heat transfer properties has been a subject of investigation for over sixty years. Various geometries and designs have been examined in these studies, such as bubble

column reactors [5], multi-phase contactors [6], horizontal pipes [7], and stirred tanks [8]. The intricate nature of dispersion behavior has prompted extensive research into heat transfer studies of such systems, with the aim of enhancing comprehension of the phenomenon.

The presence of gas in the pores of liquids within a well constitutes a fluid exhibiting two-phase flow, which has a notable impact on the characteristics of heat transfer. These blends are incorporated into a refinery system through a series of multi-pass heat exchangers and CDU pump around heat exchangers. The escalation of gas phase fraction in two-phase flows has been observed to diminish the rate of heat transfer [6], [8], [9], thereby posing a significant obstacle in the realm of energy conservation.

The presence of particles such as drops, bubbles, and solids within a liquid stream has a significant impact on various factors including the thermal conductivity of the liquid, the interaction between different phases and the wall, and the turbulence levels both within the bulk and in the vicinity of the wall. This factor has an impact on the efficiency of heat transfer in the equipment and the operational expenses associated with the process. The heat transfer rate in a processed fluid can be affected by the presence of fine solid particles, which is contingent upon the thermal properties of the dispersed particles and the hydrodynamic conditions. Some studies have reported an improvement in heat transfer enhancement, while a reduction in heat transfer has been observed under specific operating conditions. Consequently, it is imperative to thoroughly examine and delineate the various states of a system in order to gain a more profound comprehension and achieve efficacious equipment development. Nanotechnology is widely regarded as a promising technological advancement for augmenting the rate of heat transfer. In instances such as this, it is common practice to disperse nano-scale materials possessing high thermal properties into the processed fluid. This serves to enhance the fluid's thermal conductivity and augment its interfacial area, thereby facilitating superior energy management and recovery outcomes.[10]–[13]. Nano-fluids refer to solutions of nanoparticles that serve as a working fluid within heat transfer equipment, including but not limited to heat exchangers and automobile radiators. Nano-fluids have been widely utilized by researchers to increase the rate of heat transfer in single-phase systems. There is a paucity of literature on the utilization of nano-fluid for augmenting heat transfer in two-phase flow, as evidenced by the limited number of studies conducted on this topic. Complex hydrodynamic and heat transfer phenomena are anticipated in such systems, which merit thorough investigation and analysis.

The phenomenon of gas-liquid dispersion resulting in a two-phase flow occurs when gas bubbles are introduced into a liquid medium. This process is commonly observed in various industrial applications, including but not limited to fermentation processes, mixing of air with oil in the petroleum industry, cooling processes of equipment with high heat transfer requirements such as bioreactors with exothermic reactions, rockets, and nuclear reactors [14]. Gas-liquid dispersion is exemplified by the introduction of air into mixers or bubble columns for biochemical processes. The flow pattern, physical characteristics, and hydrodynamic properties of gas-liquid dispersion are contingent upon a range of parameters, including the flow rate and physical properties of the liquid [15]. Applied The occurrence of bubbles in the vicinity of a heating tube wall is facilitated by the heat flux, which induces a localized increase in temperature and subsequent boiling. This phenomenon has been observed in previous studies, where bubbles were found to form in close proximity to the wall surface. [16]The formation of gas bubbles occurs under adiabatic conditions. The features of biphasic flow can be delineated as the augmentation in the rate of heat transfer, which may escalate the likelihood of the emergence of two-phase flow. The hydrodynamic properties of fluid exhibiting streamline behavior are subject to modification due to the influence of interactions arising from the coexistence of two distinct phases. The reduction in pressure during operation results in the generation of larger bubbles within the operational segment, thereby impacting the heat transfer process in a similar manner, as previously noted in references [14] and [16]. This demonstrates the intricacy linked with the thermodynamics of gas-liquid dispersion in two-phase flow. Furthermore, local points of two-phase flow may exhibit complexities, hydrodynamic instability, and deviations from thermodynamic equilibrium between the two phases.

In order to address the intricacies involved, it is necessary to conduct experimental investigations and analysis to estimate the thermal and hydrodynamic behavior of two-phase flow [14]. Gas-liquid dispersed flow is characterized by the presence of small bubbles that are separated by a continuous phase. The present study illustrates a flow pattern wherein a low gas superficial velocity is injected into the liquid phase, which serves as the continuous phase.The phenomenon of dispersed phase flow is observed in both stationary and flowing systems of a continuous phase. The dynamic stability of various factors such as bubbles breakage, coalescence, bubble size, and interfacial area are constrained by distinct parameters [17]–[20]. The interaction between bubbles and the liquid phase, as well as the phenomena of bubble breakage and coalescence, are significant factors in the study of transport phenomena in gas-liquid dispersions [17]-[22]. The hydrodynamics of dispersed gas-liquid flow is commonly investigated through the observation of bubble coalescence and breakage. Prior research has investigated the impact of distinct operational variables on the hydrodynamics of bubbles within the continuous phase, specifically the liquid phase. These variables include the viscosity of the liquid phase, the flow rate of the liquid phase, the flow rate of the gas phase, the presence of solid particles in three-phase reactors, and the agitation speed for stirred tanks. [17]–[19]. The phenomenon of bubbles breakage is characterized by the rupture of larger "mother" bubbles into smaller "daughter" bubbles due to the influence of both internal and external forces, as described in previous literature [17-19, 23].

The impact of two-phase flow of air-water and air-oil on the heat transfer coefficient in coiled and jacketed agitated tank was examined by Rao and Murti [1973] [24]. The dimensionless groups' correlations for heat transfer enhancement in the presence of two-phase flow were obtained by the authors. The study revealed that, in general, there is an increase in heat transfer as the agitation speed for coil increases, whereas a decrease in heat transfer is observed for jacketed agitated tanks. The impact of liquid phase physical properties on heat transfer coefficient in a bubble column was investigated by Abid et al. [2015] [17]. Various liquids, including water, water with 60% ethanol, water with 35% glycerol, and water with 65% glycerol, were utilized in the study. The researchers arrived at the conclusion that the size of bubbles is influenced by various factors such as surface tension, viscosity, thermal conductivity, and specific heat, which are all dependent on the type of liquid. Liquids with higher viscosity were observed to produce larger bubbles, leading to an increase in the heat transfer coefficient. Conversely, liquids with lower viscosity were found to generate smaller bubbles, resulting in a decrease in the heat transfer coefficient[25]. The study conducted by Kashinsky et al. [2014] [26] examined the heat transfer of two-phase flow in an inclined smooth channel, covering a variety of superficial liquid and gas velocities. The present study aimed to investigate the heat transfer coefficient and shear stress at various locations within a channel experiencing two-phase flow. The results indicate a noteworthy reduction in the rate of heat transfer as the superficial liquid velocity is increased across various inclination angles. In their study, Dizaji and Jafarmadar [27] examined the impact of gas-liquid dispersion in a bubbly flow within a horizontal double pipe heat exchanger. Specifically, they introduced air bubbles into a stream of water and analyzed the resulting effects. The findings indicated that the heat transfer process was augmented when gas bubbles were present. The augmentation of heat transfer was found to be inversely proportional to the increase in Reynolds number. Additionally, it was observed that the introduction of bubbles in the shell side resulted in a greater enhancement of heat transfer as compared to the tube side. The introduction of bubbles within a tube serves as an insulating mechanism, whereas the injection of air bubbles within the shell side promotes turbulence[28]. A correlation for heat transfer of two-phase flow in a horizontal pipe was proposed by Kim and Ghajar [2006] [3]. The experimental section was exposed to a heat flux varying from 3,000 to 10,600 w/m^2, with a corresponding Reynolds number range of 820 to 26,000. The gas Reynolds number range was found to be between 560 and 48,000. The findings indicate that there is a positive correlation between the heat transfer coefficient and the liquid Reynolds number. However, the relationship between the heat transfer coefficient and the gas Reynolds number is complex and dependent on the flow pattern of the gas-liquid dispersion. The impact of agitation speed and gas flow rate on the heat transfer coefficient for a jacketed agitation tank was examined

by Xu et al. [1997] [29]. A correlation of significant complexity was noted between the agitation velocity, gas flow rate, and heat transfer coefficient. A reduction in heat transfer was noted when the critical gas flow rate exceeded 4 m3/hr at an agitation speed of 300 rpm. An increase in heat transfer efficiency was noted when the agitation speed was maintained below 200 rpm. The prediction of entrained liquid fraction in adiabatic gas-liquid annular two-phase flow in vertical pipes was examined by Cioncolini and Thom in 2010 [30]. This study has evaluated nine empirical correlations using an experimental data bank consisting of 1504 data points for 8 distinct gas-liquid combinations and 19 tube diameters ranging from 5.00 mm to 57.1 mm. The study determined that the correlation between Sawant, Ishii, and Mishima and that of Oliemans, Pots, and Trompé yielded the most accurate representation of the available data. A novel methodology for correlation, which was developed based on physical intuition and dimensional analysis, has been suggested. This approach has demonstrated superior performance compared to the existing techniques and has the potential to offer additional physical understanding of the atomization process of liquid films. The recently proposed correlation is founded upon the Weber number of the core flow, which is a crucial dimensionless parameter in ascertaining the wall shear stress and the corresponding frictional pressure gradient of annular flows. In 2014, Vidal [31] proposed a no-slip technique for forecasting the friction factor and, by extension, the frictional pressure drop in instances of two-phase flow. The proposed methodology, which relies on the redefinition of the mixture Reynolds number, exhibits superior precision in comparison to other techniques documented in the literature. Nonetheless, the aforementioned approach failed to incorporate pertinent two-phase flow data due to the homogeneous assumptions made. The present investigation involves the manipulation of the mixture Reynolds number by incorporating the characteristics of two-phase flow phenomena, specifically the void fraction and flow pattern parameters. The study utilized data that was publicly accessible in scholarly publications to conduct a comparative analysis between theoretical predictions and empirical observations. The present study analyzed various flow regimes in the context of biphasic horizontal flow of refrigerants and air-water mixtures. The predictions generated by the proposed method were subjected to comparison with a pre-existing model from the literature and other homogeneous methods. The results of the comparison validated the superior accuracy of the new predictions. This manuscript provides a comprehensive account of the enhanced friction factor technique.

The improvement of heat transfer in industrial processes has become an increasingly pressing challenge due to economic and safety considerations. The investigation of the heat transfer phenomenon in solid-liquid dispersion systems, also known as nano-fluids, is a crucial area of interest for researchers in order to facilitate the effective design of heat exchangers. The utilization of nanotechnology has been recognized as a noteworthy approach to improve heat transfer. This involves the dispersion of materials at the nano-scale into the process fluid, which serves to enhance the thermal conductivity of the working fluid [11]-[13].The introduction of nanoparticles into the process fluid is a method employed to augment heat transfer by elevating the heat transfer coefficient in situations where forced convection is present. According to reference [32], enhancing the dispersion of high conductivity nanoparticles in a fluid leads to an augmentation of the heat transfer coefficient, thereby improving the heat transfer characteristics. The physical characteristics of the process fluid, including viscosity, density, heat capacity, and flow conditions, are also influenced by the dispersion of nanoparticles. The thermal conductivity of nanoparticles is contingent upon various factors, including temperature, nanoparticle size, pH, and nanoparticle concentration [33]. The static model of thermal conductivity postulates that nanoparticles remain immobile within the bulk fluid, which in turn exhibits a uniform distribution of nanoparticles. This fluid flows in a streamlined manner within the bulk fluid, as per reference [34]. The correlation between dynamic models and assumptions of random movement of nanoparticles within bulk fluid has been observed. However, the presence of flow turbulence has been found to deform the stream line flow structure and result in non-uniform distribution of nanoparticles, as reported in previous studies [33], [35]. The impact of nano-fluids on the dispersed flow's heat transfer rate has been the

subject of extensive research over the past few decades. The present investigations have employed nanoparticles, which are classified as solid materials of nano-scale dimensions, while being suspended in a large volume of fluid. This section provides an overview of prior research that is pertinent to the current study. Several studies that have been previously documented comprise:
In their study, Duangthongsuk and Wongwises (2009) [36] utilized TiO2 nanoparticles with a diameter of 21 nm and a concentration of 0.2 vol% to augment heat transfer within a horizontal pipe. This approach aimed to improve the efficiency of heat transfer in the system. The findings indicate that an improvement of 6-11% was achieved, and the heat transfer coefficient exhibited an upward trend as the flow rate of the hot fluid increased, while it decreased as the temperature of the nano-fluid rose. The findings of the study indicate that the utilization of nano-fluid does not yield any noteworthy impact on the pressure drop. Moreover, the friction factor of the nano-fluid was found to be in close proximity to the friction factor of water in the absence of nanoparticles. The study conducted by Zamzamian et al. [2011] [32] investigated the augmentation of heat transfer in a heat exchanger through the utilization of CuO/ethylene glycol and Al2O3/ethylene glycol nano-fluid. The study examined forced convection heat transfer and analyzed the impact of nanoparticle size, concentration, and temperature. The findings demonstrated a high level of concurrence with previously established correlations. The findings of the study suggest that there is a positive correlation between the concentration of nanoparticles and temperature with an increase in heat transfer coefficient by 2-50%. In 2013, Darzi and colleagues [37] conducted an experimental study to assess the effects of a 20 nm Al2O3 nanofluid on the heat transfer, pressure drop, and thermal performance of a double-tube heat exchanger. The study aimed to determine the effective viscosity of nanofluid within a temperature range of 27 to 55 degrees Celsius. The study involved conducting experiments at different Reynolds numbers, ranging from 5000 to 20,000, while varying the concentration of nanoparticles up to 1% by volume. The findings indicate a high likelihood of enhancing the thermal efficiency of heat exchangers through the incorporation of nanoparticles within the examined parameters, provided that there is no significant increase in pressure drop. An empirical correlation was established for the alteration of the Nusselt number, taking into account the Reynolds number and the concentration of nanoparticles.b The study conducted by Aghayari et al. (2014) [38] investigated the enhancement of the heat transfer coefficient and Nusselt number in a nanofluid that consisted of gamma-AL2O3 nanoparticles with a particle size of 20nm and a volume fraction ranging from 0.1% to 0.3% (V/V). This study investigates the impact of temperature and nanoparticle concentration on variations in Nusselt number and heat transfer coefficient in a twin pipe heat exchanger with counter turbulent flow. The level of concordance between empirical observations and theoretical data derived from semiempirical equations is deemed acceptable. The results of the experiment indicate that there is a notable increase of 19%-24% in both the heat transfer coefficient and Nusselt number. It has been observed that the heat transfer coefficient increases in correlation with both the operational temperature and concentration of nanoparticles. In their study, Albadr et al. (2013) [39] incorporated Al2O3 nanoparticles with a size of 30nm and a volume percentage range of 0.3-2 vol% as an additive to the thermal fluid within a shell and tube counter flow heat exchanger. The findings indicate that the augmentation of nano-fluid volume fraction resulted in a marginal enhancement of the heat transfer coefficient. An increase in the volume fraction of nano-particles resulted in a subsequent increase in the viscosity of the bulk fluid, leading to an increase in the friction factor. The study conducted by Rostamzadeh et al. (2014) [40] aimed to investigate the mixed convection heat transfer of Al2O3-water nanofluid within a vertical, W-shaped copper-tube with a uniform wall temperature through experimental means. The experiments encompassed various intervals of complex variables such as Reynolds number, temperature, and volume fraction of particles. The findings indicate that an increase in Reynolds number led to an enhancement in the heat transfer coefficient rate for mean wall temperatures of 50 and 60ºC. Furthermore, there was a slight increase in the heat transfer coefficient as the Reynolds number increased. Remarkably, the pressure differential of the nanofluid exhibited a proximity to that of the base fluid. Additionally, a novel correlation has been suggested for the computation of the Nusselt number within W-shaped tubes.

Due to the unpredictability of gas-liquid dispersion/nano particle interactions, research into the increase of heat transfer by employing nanofluid under two-phase flow gas-liquid dispersion is uncommon. Not much is known about how fine gas bubbles affect heat exchanger efficiency from publicly available sources. This study utilizes a double-pipe heat exchanger in order to examine the impact of air bubble dispersion in water on the heat transfer coefficient under varying gas and liquid flow rates. The use of copper oxide nanoparticles to improve heat transfer in gas-liquid mixtures is another area of investigation.

2. Experimental Work

To illustrate the experimental setting, see Figure1. A double-pipe heat exchanger, agitated tank, coiled heater, water chiller, pumps, control valves, annular-type flow meters (rotameters), temperature data-logger, air pump, and U-tube manometer were all part of the experimental setup. The gas-liquid mixture was dispersed by inserting it into an agitated tank with 8 flat blade impellers (Rushton turbine). The impeller has a diameter of 60 mm with a blade that is 25 mm in length, 10 mm in breadth, and 3 mm in thickness.

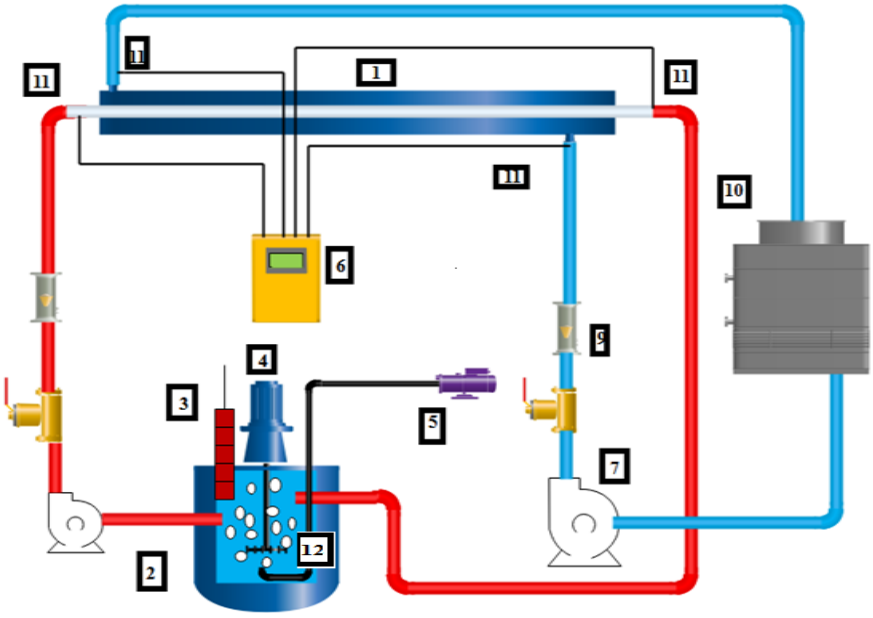

Figure 1: Schematic diagram of experimental rig.

1.Double pipe heat exchanger, 2. Agitated tank, 3.Coiled heater, 4.Agitator motor, 5.Air pump, 6.Temperature data-logger, 7. Centrifugal pump, 8. Control valve, 9. Rotameter), 10.Chiller, 11.Thermocouples, 12.Impeller.

The first stage of the tests consisted of determining the total heat transfer coefficient (Uo) for single phase using water as the working fluid in the tube (tube side) and annulus (shell sid) throughout a range of Reh (19900-64000) and Rec (4750-13100). The water in the agitated tank was heated to 43 degrees Celsius using a coil heater, and then cooled to 15 degrees Celsius using a chiller. A centrifugal pump was used to transfer hot water into the heat exchanger's tube side, while a separate pump sent cold water into the heat exchanger's shell side. The hot and cold water flows were controlled by control valves. Using annular flow meters, we were able to calculate a hot Reynolds number (Reh) of 1900–64000 and a cool Reynolds number (Rec) of 4550–13100 for the flows. With a data-logger recording temperatures and an inverted manometer measuring pressure drop, we determined how the heat exchanger performed throughout a range of Reynolds numbers.

The data logger recorded the intake and output temperatures of both fluids on an excel sheet inside a ram that was included within the device. Each of the three experimental components relied on the temperatures to calculate heat transfer rate, log mean temperature difference, and an overall heat

transfer coefficient. Each time a temperature reading was taken (every 5 seconds), the data logger would save it. After each test run was completed, the temperature was recorded for another 5 minutes. For this reason, we took 60 temperature readings at the beginning and end of each run. At least two separate runs were taken. In order to guarantee the reliability of the findings, each measurement was repeated 120 times. As a benchmark, we looked at the mean average.
It was determined how to compute the total heat transfer coefficient using the outside surface area of the inner tube.

$$Q = \dot{m}_h Cp_h(T_{hA} - T_{hB}) = \dot{m}_c Cp_c(T_{cA} - T_{cB}) \quad (2)$$

$$\overline{\Delta T} = \frac{(ThB-TcB)-(ThA-TcA)}{\ln(\frac{(ThB-TcB)}{(ThA-TcA)}} \quad (3)$$

$$U_o = \frac{Q}{A_{So}\overline{\Delta T}} \quad (4)$$

The frication factor was calculated from pressure drop measurements for tube side as:

$$f = \frac{\Delta p}{2\rho.U\infty^2}\frac{d}{L} \quad (5)$$

Part two of the trials included achieving dispersion by the introduction of air bubbles into an agitated tank that was being mixed by an 8-flat blade impeller spinning at either 200 or 800 revolutions per minute. When the impeller spins, it causes air bubbles to break apart and scatter their fine offspring farther and wider. The water in the test portion was kept at 15 degrees Celsius, and a hot dispersion fluid was injected into it to generate a temperature difference of 43 degrees Celsius.
The shear force of the impeller in the tank fractured the injected air bubbles into smaller daughter bubbles, resulting in more dispersion. A helical heater kept the water in the tank at a constant 43 degrees Celsius. In a countercurrent flow arrangement, the gas-liquid combination was introduced into the tube side, and cold water was introduced into the shell side. The Reynolds number for the hot fluid ranged between 1990 and 64000. The water chiller supplied the annulus with water in the 4550-13100 Reynolds number range. The agitation speeds varied between 200 and 800 rpm, while the air injection rates varied between 0.054 and 0.18 m3/h.
In one set of studies, slow-motion cameras were used to observe the diffusion of gas through a liquid. The size of the daughter bubbles was extracted from the photos by comparing the size of the bubbles to a standard item and then measuring the difference in pixels. The diameter of the impeller shaft was used as the standard. An average of over 40 bubbles was used to determine the average bubble size for each scenario.
Finally, copper oxide nanoparticles with the characteristics listed in Table 1 were included. The method used was the same as that outlined for the single-phase experiment. Concentrations of nano-fluid (from 0.5 g/l to 3 g/l) were created by adding copper oxide (CuO) nano-particles to boiling water. Under controlled conditions, the nano-fluid was heated to 43 degrees Celsius in an agitated tank. The frigid water was around 15 degrees Celsius. Nano-fluids with Reh values between 1900 and 64,000 (determined from the physical parameters of the continuous phase, water) were injected into the tube side of the heat exchanger, maintaining a constant Rec of 9,000. As the conditions changed, the tube's temperature and pressure decrease were recorded. Table 2 displays the characteristics of nanoparticles under typical operating circumstances.

Table 1:Properties of copper oxide nanoparticles.

size, nm	Purity %	Shape	Specific gravity	Specific surface area, m^2/g	Thermal conductivity, $W/m^2.K$
40	99	spherical	6.4	120	32.8

The number of bubbles per unit time was obtained by finding average size for each injection test based on visualization analysis as:

$$\dot{n} = \frac{Q_g}{\frac{4}{3}\pi d_p^3} \tag{6}$$

Volume averaged interfacial area based on bubbles size distribution is expressed as follows [Kataoka et al, 2012]:

$$\text{a} = \frac{\pi d_p^2 n}{V} = 6\frac{\alpha}{d_p} \tag{7}$$

when a Volume-averaged interfacial area, dp (the diameter of the mother and daughter bubbles as determined by the visualization research), (the void %), n (the number of bubbles), and V (the volume of the container). The volume of the liquid did not change much despite the pumping of air into it. hence, Eq. took into account just the volume of the single phase (water) (7(
The following expreaaions were used to demonstrate how to compute the standard deviation and confidence levels for use in statistical analysis:

$$\text{S} = \left(\sum(\overline{U_o} - U_o)^2 \frac{1}{n_{exp.}-1}\right)^{0.5} \tag{8}$$

$$\text{Cl} = \overline{U_o} \pm \text{S} \times \frac{z}{n_{exp.}{}^{0.5}} \tag{9}$$

The ensuing dispersion from the mean values of the total heat transfer coefficient is quantified by its standard deviation. The margin of error quantifies the range of possible errors. The results of the statistical evaluation of the current work's four sections are shown in Table 2.

Table 2: Averaged standard deviation and margin error of 90% degree of confidence of for all experimental conditions.

Parameter	Single phase	Gas-liquid dispersion	Nano-fluid	Gas-nano-fluid dispersion
Stdev of U_o , W/m^2.k	51	From 48 to 50.9	49.35	52.31
Margin of error of U_o of 90% degree of confidence, W/m^2.k	±18.8	±18.3	±18.2	±19.3

3. Results and Discussions

3.1. Bubbles breakage visualizations

The slow-motion video camera was used for the visualization. When analyzing the experimental data, the size of the bubbles was determined by comparing the picture pixels to the impeller shaft. In a gas-liquid dispersion flow, the heat transfer properties are heavily influenced by the bubble size and distribution. Figure2 illustrates that the size of the mother bubble and the number of bubbles per second are both functions of Qg. The creation rate of daughter bubbles depends on both Qg and N. As seen in Figures 3 and 4, a mixer was utilized to increase the rate of dissipation of energy, so encouraging the breaking and spreading of bubbles. Figure 3 displays the relationship between bubble diameter (dp) and agitation speed (N) over a range of Qg. Due to the constant generation of smaller daughter bubbles produced by the fragmentation and breaking of mother bubbles, dp typically decreases as N increases. Liao and Lucas [2009], Solsvik and Jakobsen [2015], and Hasan [2017b] are all corroborated by the visualization findings. As shown in Figures 4 and 5, the interfacial area of gas-liquid dispersion grows as N rises because the bubbles generate smaller pieces for the same gas flow rate. In bubbly dispersed flow, a greater gas flow rate (Qg) results in a greater number of fragments per second and a greater interfacial area between the gas and liquid

phases. According to Hasan, [2017b], a larger gas flow rate increases the number of mother bubbles in the test section, which in turn raises the risk of bubbles breaking. This holds true for a range of values of N.

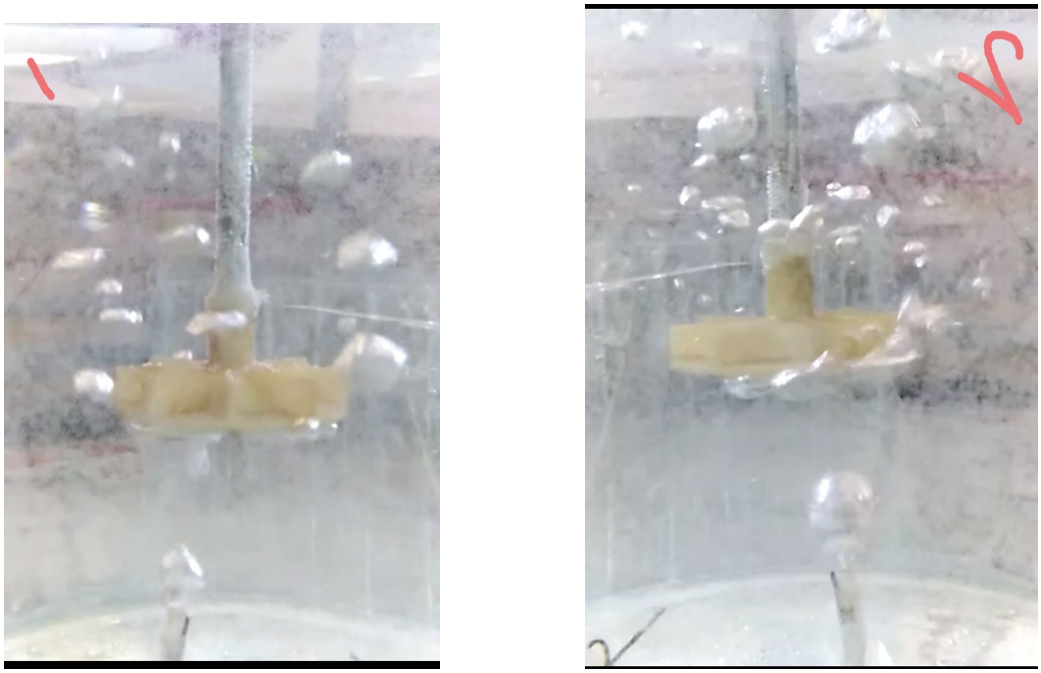

a. N=0 b. N=200 rpm

Figure 2: Bubbles breakage by utilizing d_i= 60 mm impeller and Q_g=0.054 m^3/h for various N.

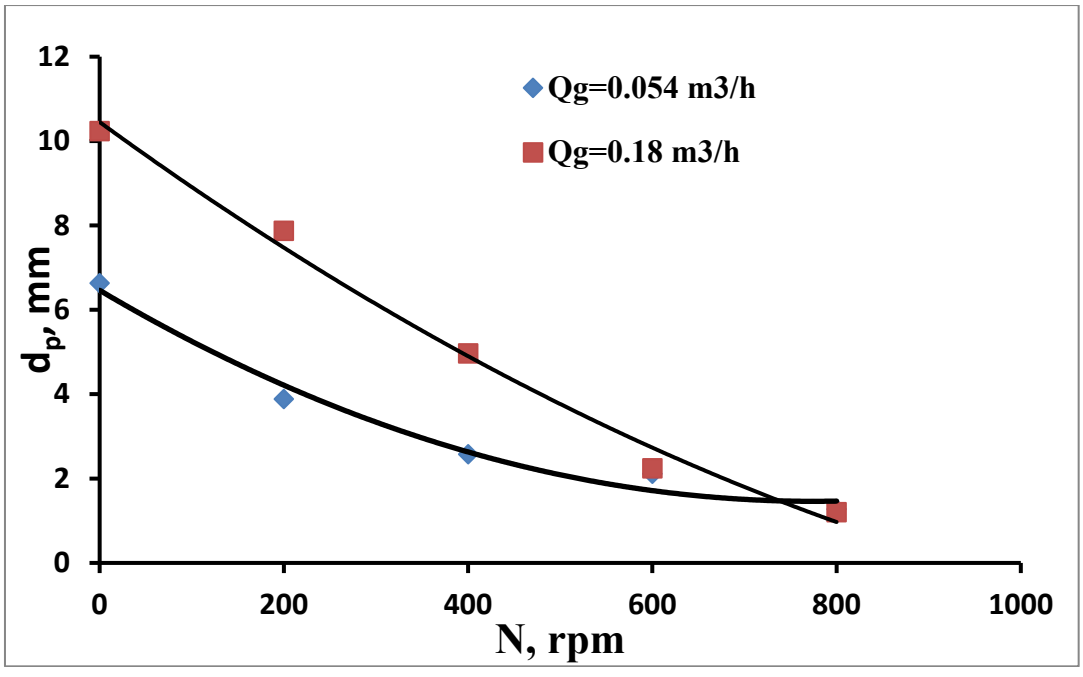

Figure 3: Bubbles diameter vs. agitation speed for various Q_g.

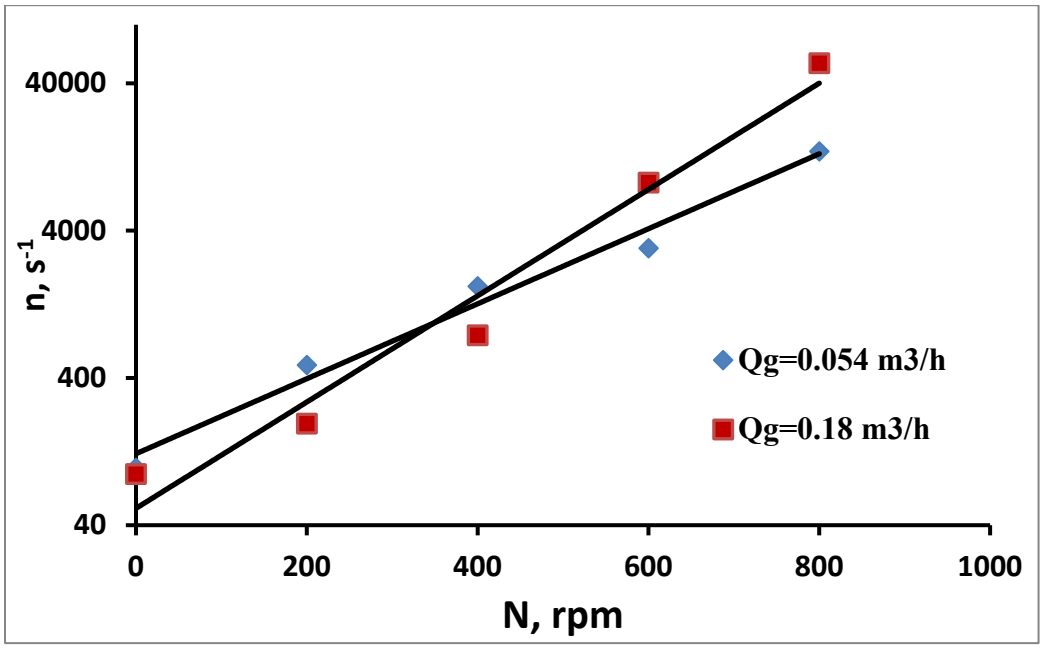

Figure 4: Number of bubbles number per time vs. Agitation speed for various Q_g.

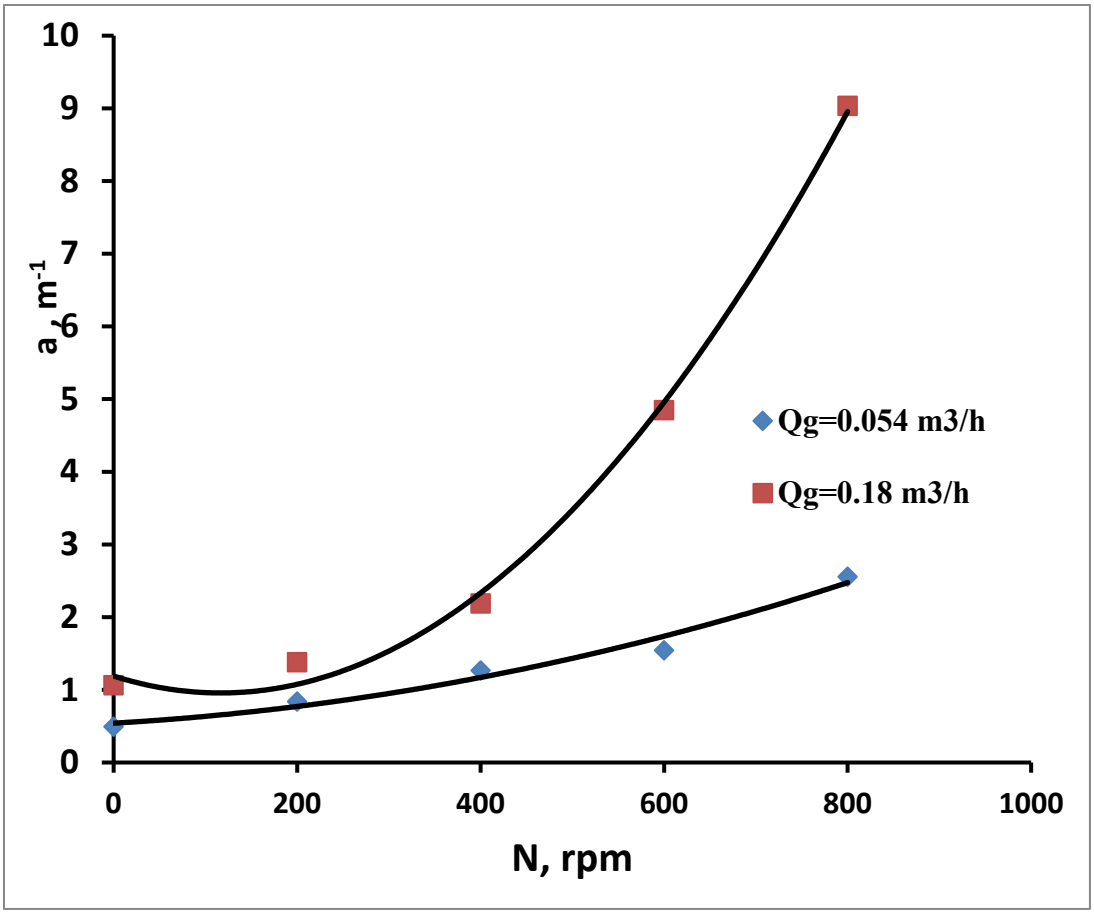

Figure 5: Interfacial area vs. agitation speed for various Q_g.

3.2. Heat transfer coefficient

Figure 6 shows the global heat transfer coefficient vs Reh for a range of Rec values for single-phase flow. When both Reh and Rec are raised, the total heat transfer coefficient rises. For both hydrodynamic and thermal boundary layer degradation, a high Reynolds number is responsible [Brodkey and Hershey, 1988; Slaiman et al., 2007]. Turbulent eddies are created when a high Reynolds number is reached. Figure 7 demonstrates that the results from the current study accord well with the results from Dittus and Boelter's [1930]correlation for Rec=9000.

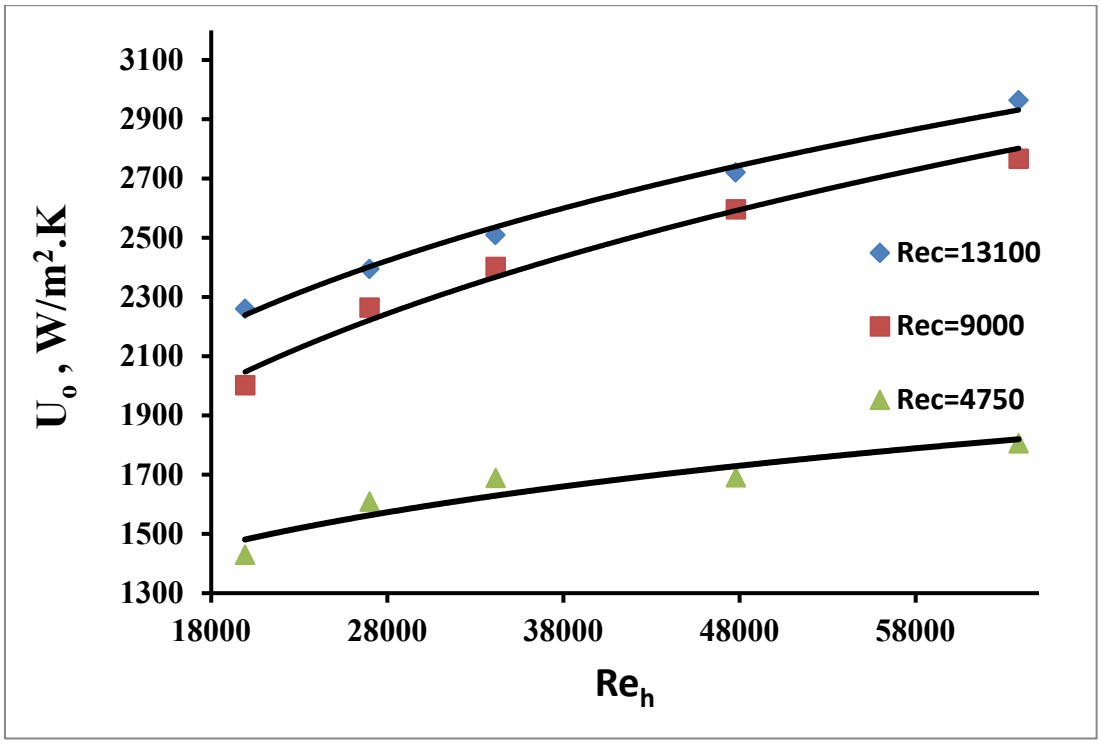

Figure 6: Overall heat transfer coefficient vs. Re_h for various Re_c for single phase flow.

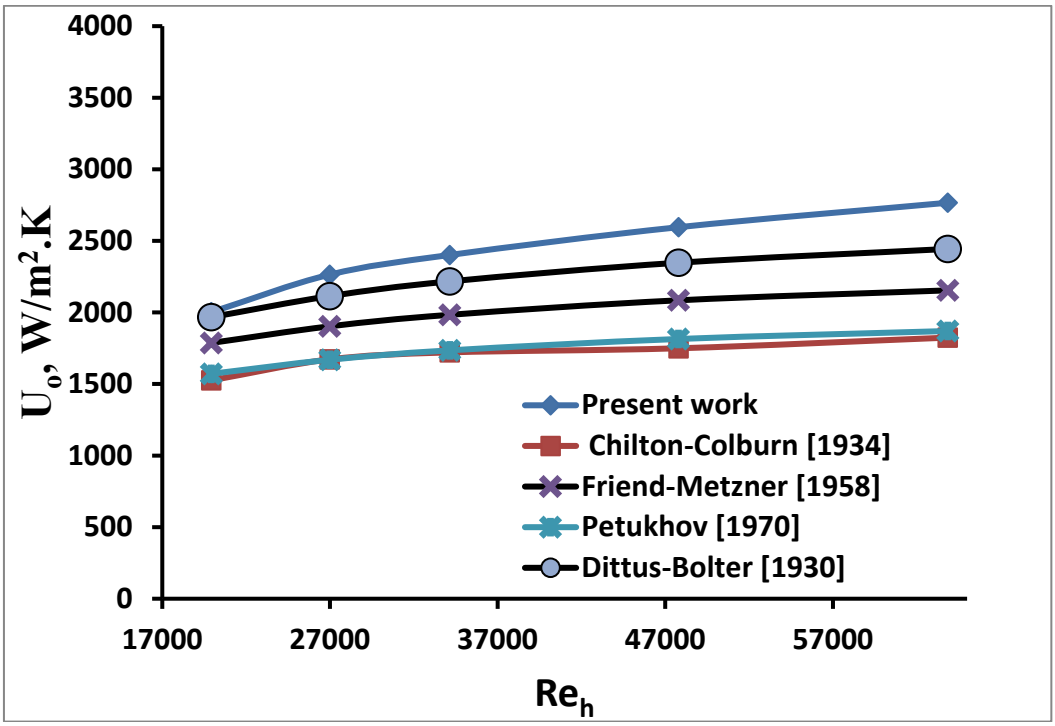

Figure 7: Overall heat transfer coefficient vs. Re_h for single phase flow and previous work correlation of Re_c=9000.

For di=60 mm impeller and Qg=0.054 m3/h, as shown in Figure 8, the influence of Reh on the f factor for gas-liquid dispersion flow can be seen. Figure 8 shows that for different values of N, ffactor has an inverse relationship with the Reynolds number. At higher N, when smaller bubbles are produced, the friction factor is less. Since the smaller bubbles spend more time in contact with the medicine, the viscous forces of the stream lines are also reduced. Pressure loss and friction are both reduced under flowing circumstances as a consequence of the material's increased density and viscosity [Saffariet al., 2013]. At N=800 rpm and Re=30000, the friction factor decreases by around 25%.

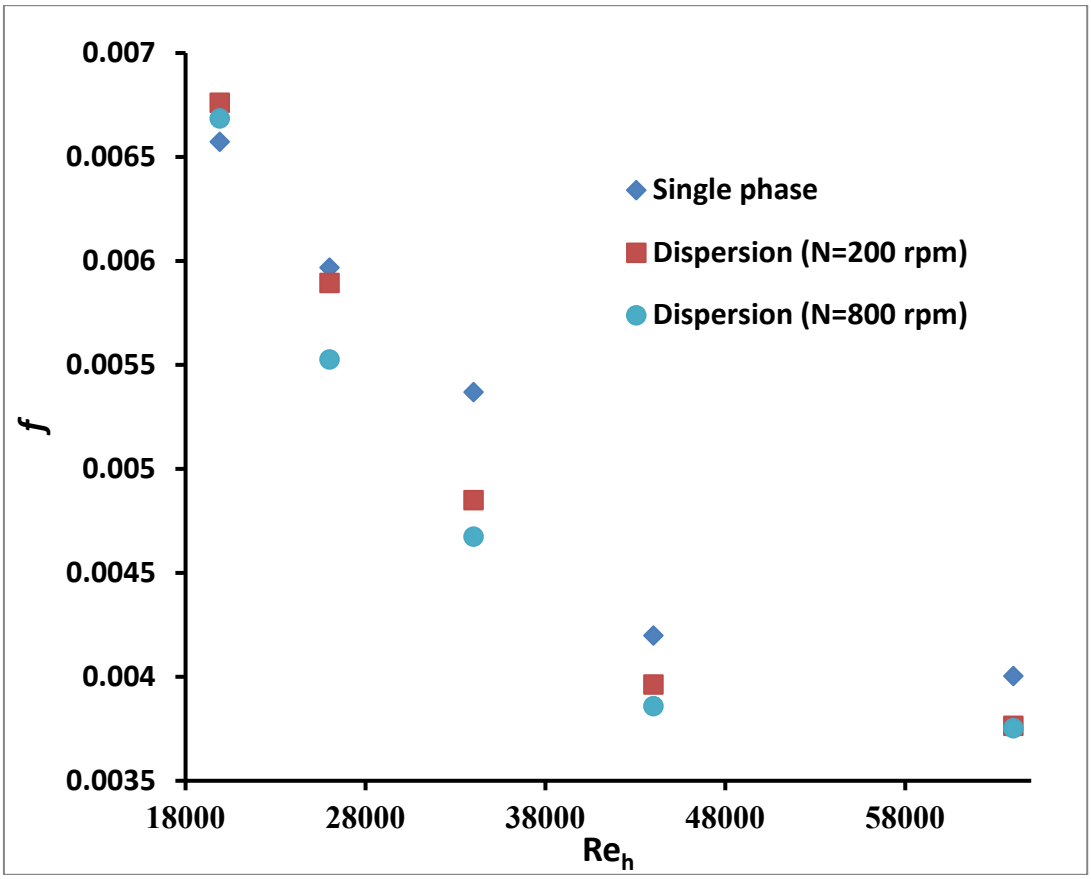

Figure 8: Friction factor vs. Re_h for gas-liquid dispersed phase flow for various of N when d_i=60 mm and Q_g=0.054 m^3/h.

A gas-liquid dispersion system is shown in Figure 9 with di=60 mm, Qg=0.054m3/h, and different agitation speeds. Uo tends to rise when Reh rises because of the aforementioned enhancement in convective heat transfer. While under stress, Uo does not always follow the same pattern as Reh. This is because the thermal characteristics of the continuous phase and the turbulence level are affected by the complex behavior of bubble rupture and coalescence. It can be shown that the Uo for a single phase (water) is greater than the dispersion for weak to moderate Reh. Uo for dispersion is greater for high Reh and comparatively high N. The behavior of the heat transfer coefficient in an agitated gas-liquid dispersion is complicated. For all values of N, heat transmission improves with rising Reh and then declines between Reh=27,000 and 37,000. Once Reh is over 37,000, the heat transfer coefficient begins to rise, eventually surpassing single-phase values at Reh>47,000. Xuet al. [1997] found a similar pattern of behavior in a system like this.

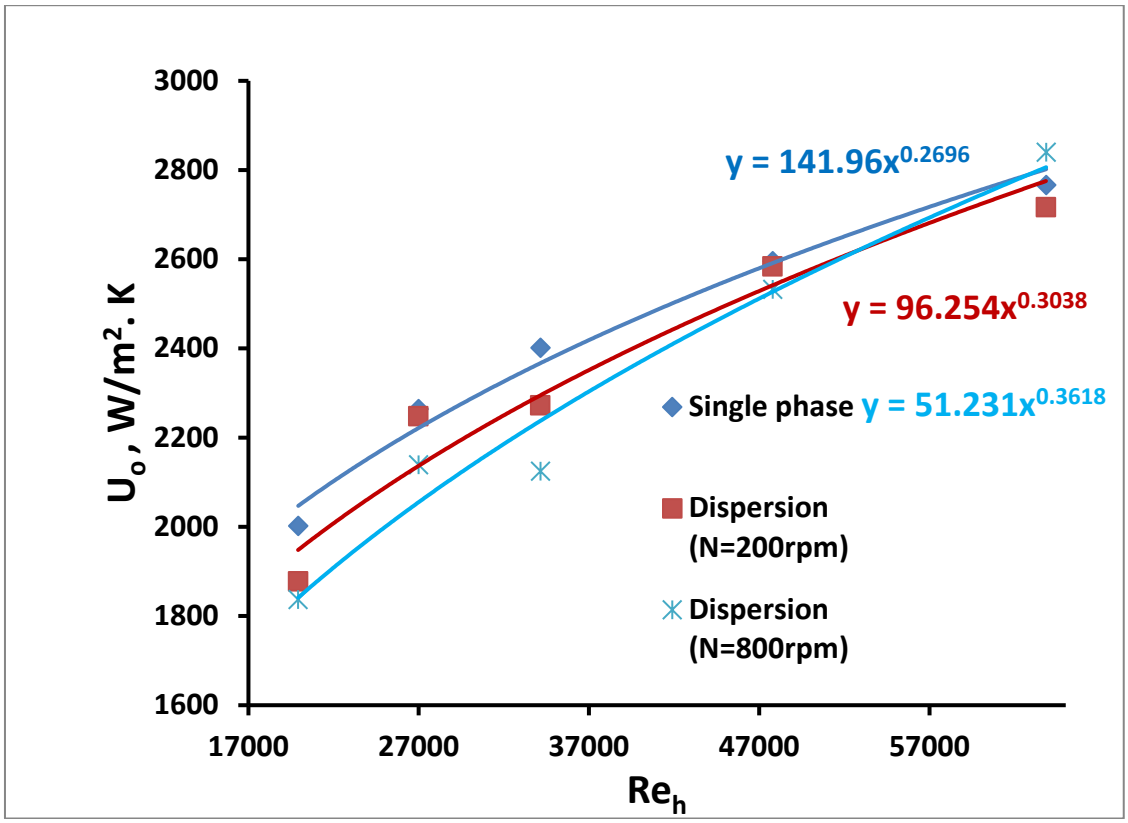

Figure 9: Overall heat transfer coefficient vs. Re_h for various N of gas-liquid dispersion at Q_g=0.054m^3/hat Re_c=9000.

For di=60 mm and Qg=0.181 m3/h in a gas-liquid system, the relationship between Uo and N is shown in Figure 11. At Reh=64000, the optimum agitation speed is N=800 rpm and the smallest Uo is recorded over the whole range of Reh. A fluctuating agitation speed, as measured by Uo, reveals the rates of fragmentation and coalescence under these varied operational settings. This intricate pattern of N's impact on Uo is influenced greatly by bubble size. When N is low, huge bubbles rise more quickly than the smaller bubbles created when N is high. Increases in N cause a greater proportion of bubbles to burst, with the result that more turbulence is generated and more heat transferred [Rao and Murti, 1973].

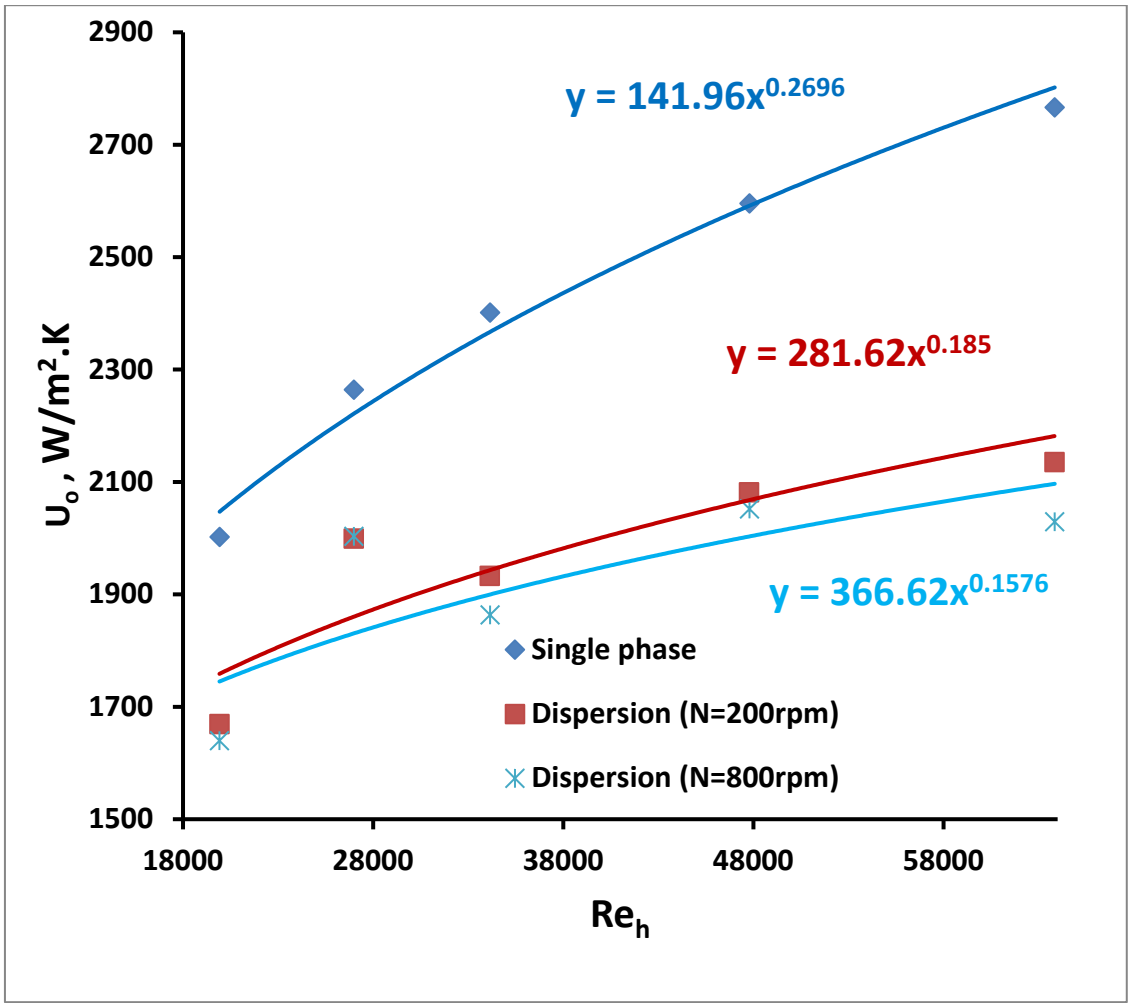

Figure 10: Overall heat transfer coefficient vs. Re_h for various N of gas-liquid dispersion at 0.18 m^3/hat Re_c=9000.

If di=60 mm and Qg=0.0545 m3/h is entered into the gas-liquid system simulator, the resulting plot is shown in Figure 11. At Reh=64000, the optimum agitation speed is N=800 rpm and the smallest Uo is recorded over the whole range of Reh. The rates of fragmentation and coalescence under these various operating settings are shown by the non-uniform trend of agitation speed in Uo. This intricate pattern of N's impact on Uo is influenced greatly by bubble size. When N is low, huge bubbles rise more quickly than the smaller bubbles created when N is high. As N rises, more bubbles rupture, with smaller bubbles inducing more turbulence while larger bubbles consolidate to improve the heat transfer coefficient [Rao and Murti, 1973].

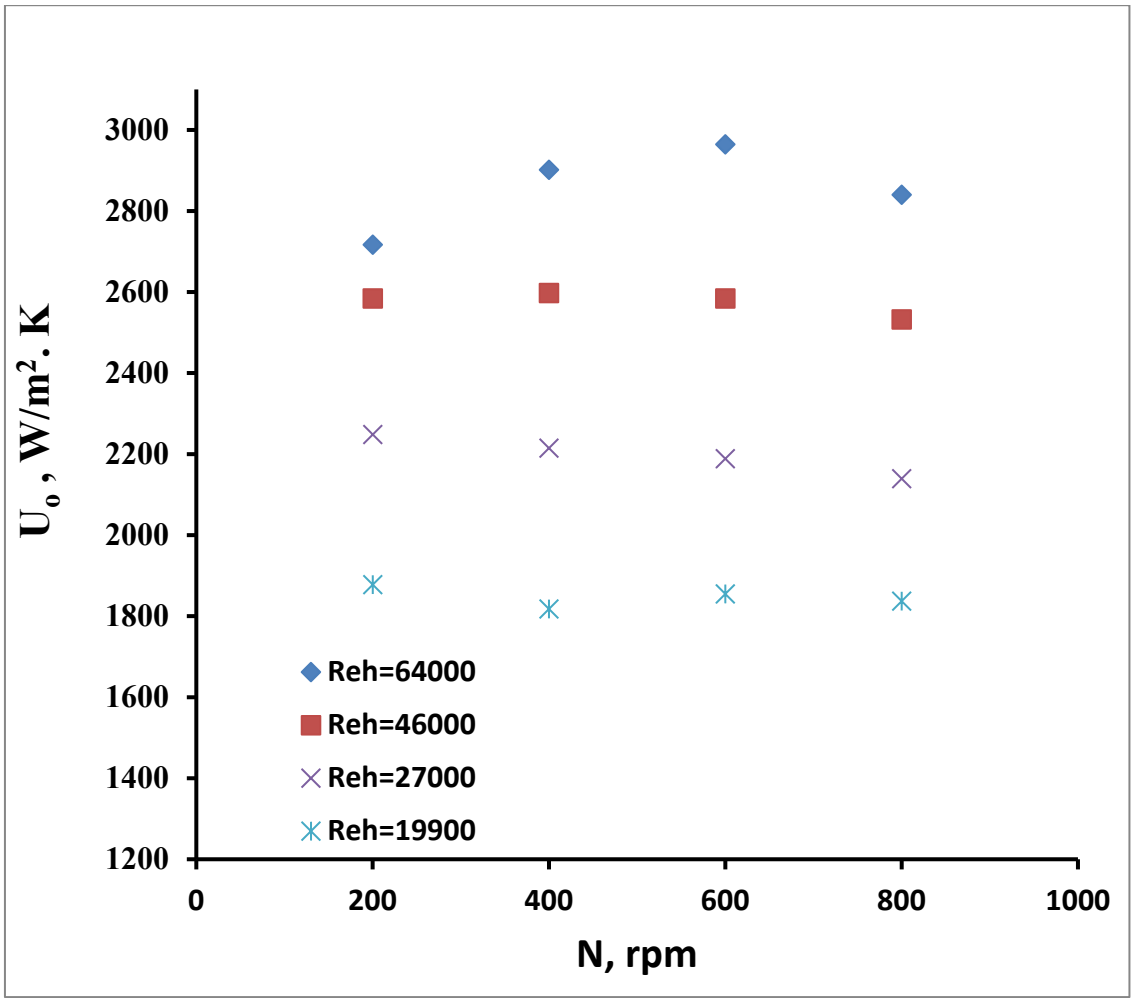

Figure 11: Overall heat transfer coefficient vs. agitation speed for various Re_h of gas-liquid dispersion at Q_g=0.0545m^3/hand at Re_c=9000.

3.3. Forced convection of nanofluid

The friction factor (f) vs the resistance to heat transfer (Reh) of nanofluid flow inside a heat exchanger at Rec=9000 for different concentrations of nanoparticles is shown in Figure 12. (C). For a constant C, the Reynolds number has a negative effect on f. Consistent with the findings of Sahin et al. (2015), for small values of Reh, the friction factor for nanofluid is less than that for a single phase (water). For Reh >= 43000, the concentration of nanoparticles has no appreciable impact on f. This behavior is grounded on the physicochemical characteristics of nanofluid, which exhibit a modest increase in viscosity and density. This impact becomes almost nonexistent at high speeds [Bianco et al., 2015].

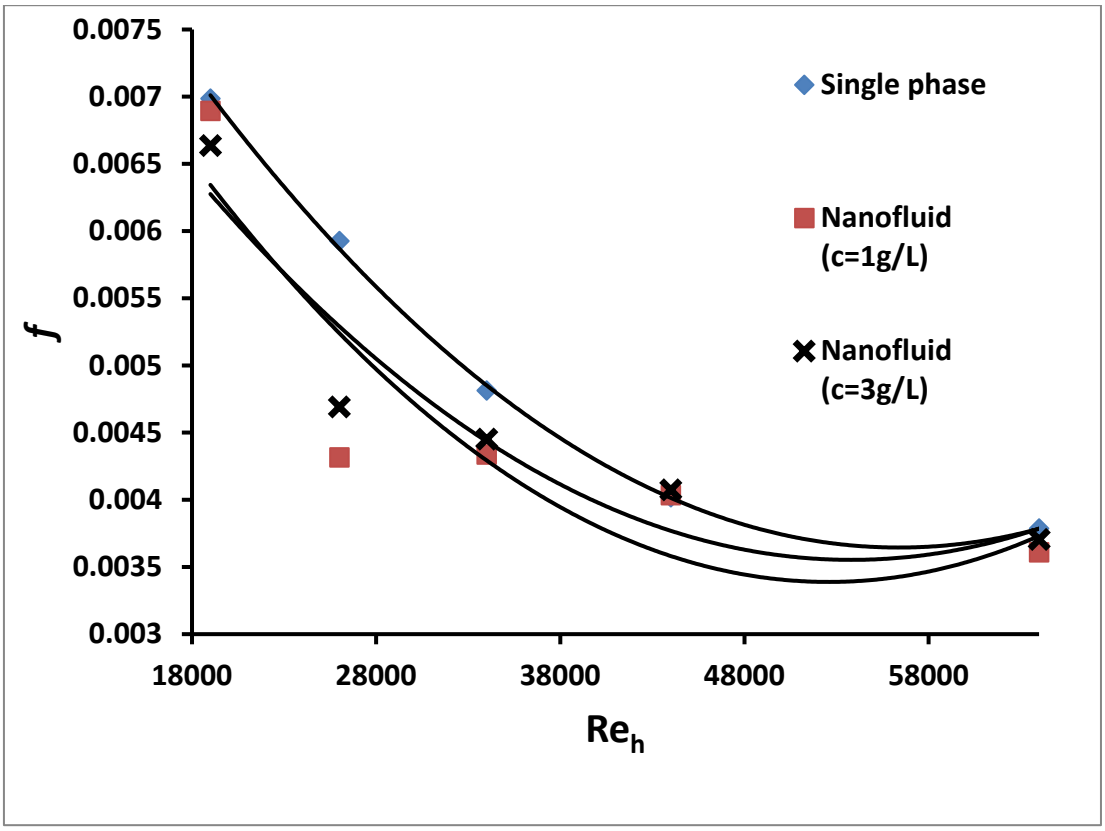

Figure 12: Friction factor vs. Re_h of nanofluid for various C.

As shown in Figure 13, as the concentration of nanoparticles rises, so does the heat transfer coefficient. According to the graph, the optimal value for enhancement at high Reh is 2 g/L, whereas at low Reh, the value is 1 g/L. For a concentration of 3 g/L, the heat transfer coefficient marginally reduces. A considerable increase in the heat transfer coefficient is seen between 0.5 and 1g/L of nanoparticles, followed by a modest rise at 2g/L and a subsequent reduction at 3g/L of nanoparticles. Coefficient of heat transmission depends on nanofluid's physical characteristics and its hydrodynamics. As nanofluid thermal conductivity rises, so does the heat transfer coefficient. As C is increased, a fouling layer of nanoparticles forms on the tube's surface, reducing heat transmission and hence lowering Uo[Sarafraz et al., 2017]. Sarafraz et al(2017) .'s findings that the heat transfer coefficient of a plate heat exchanger rises with nanofluid concentration up to 0.3% and begins to decline beyond this concentration are generally supported by the data presented here.

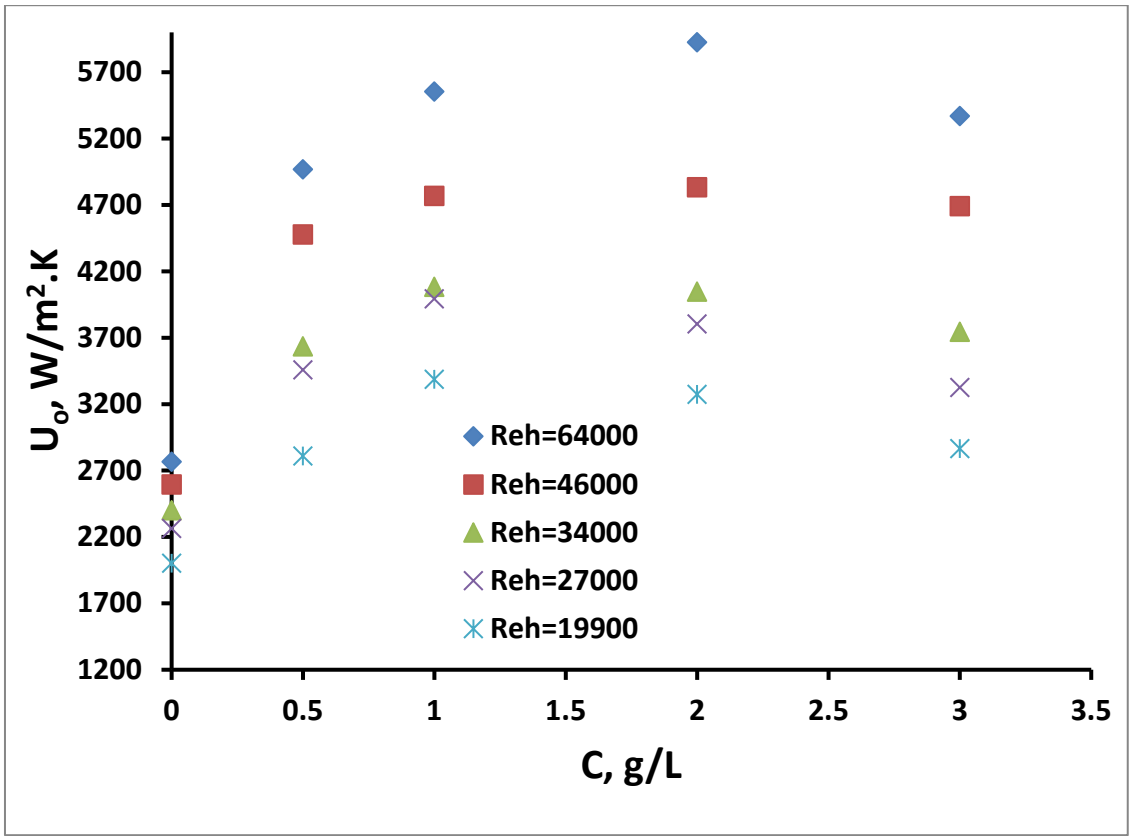

Figure 13: Overall heat transfer coefficient vs. C of nanofluid for various Re_h at Re_c=9000.

3.4. Forced convection of gas-nanofluid dispersion

Multiple graphs of the overall heat transfer coefficient versus Reh are shown in Figures 14 and 15. A higher Reynolds number improves heat transmission by a greater percentage. There seems to be no observable pattern of improvement with increasing N. As the thermal conductivity of the gas-liquid dispersion increases, the influence of tiny bubbles is mitigated, resulting in improved heat transmission. When nanoparticles are introduced, the tiny bubbles responsible for the drop in Uo are compelled to merge into bigger bubbles. Nanoparticles distort tiny bubbles into bigger ones, and their collisions create turbulent intensities that destroy the thermal boundary layer. When employing nanofluids for improved heat transmission, the rule of thermal conductivity is crucial. The mechanics of nano-scale convection are discussed by Jang and Choi [2004]. The processes employed by Jang and Choi [2004] include the collision of molecules in the liquid phase, the collision of nanoparticles, the thermal diffusion of solid nanoparticles, and nano-scale Brownian motion generated by nano-scale convection. Here we see the originality of the current study, which, in contrast to the conventional approach of applying excessive liquid pressure to suppress two-phase flow, improved heat transmission of the latter by using the nanoparticles' functional properties. Table 3 shows that the optimum heat transmission occurs at N=800 rpm and Reh=64000.

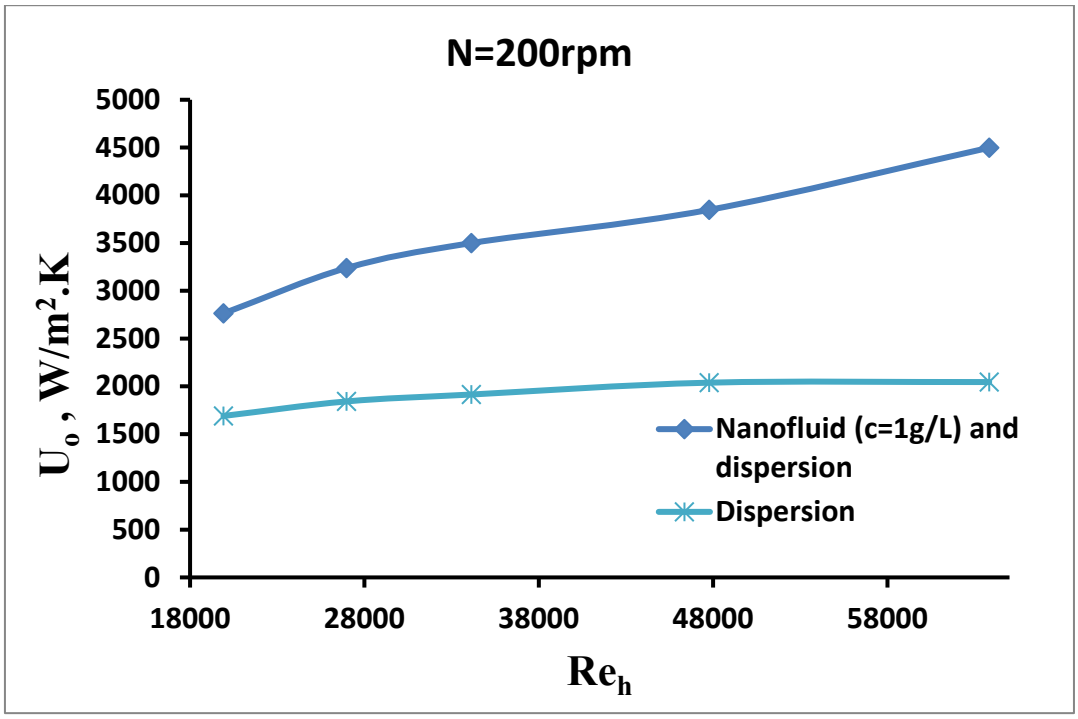

Figure 14: Overall heat transfer coefficient vs. Re_h for gas-solid-liquid dispersion (gas dispersed in nanofluid) at Q_g=0.0545 m^3/h ,C= 1g/L, N=200 rpm and Re_c=9000.

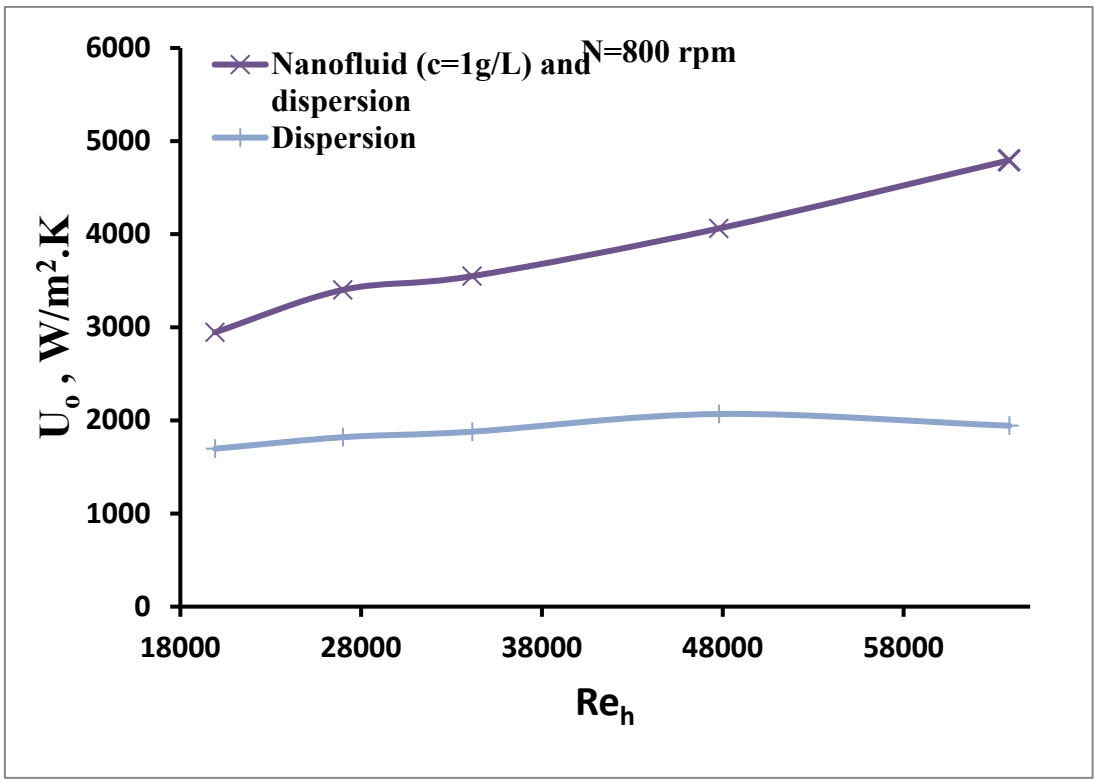

Figure 15:Overall heat transfer coefficient vs. Re_h for gas-solid-liquid dispersion (gas dispersed in nanofluid) at Q_g=0.0545 m^3/h, C= 1g/L, N=800 rpm and Re_c=9000.

4. Conclusion

Heat exchanger performance was evaluated by calculating the total heat transfer coefficient under various testing settings. Heat transfer coefficient may be considerably impacted by two phase flow interaction at higher gas flow rates for different agitation speeds (gas-liquid dispersion as a

consequence of bubbles breaking). Hydrodynamic action improves heat transfer with greater contiguous phase Re and lower gas flow rate. The heat transmission coefficient drops to its lowest value—30%—under the most severe circumstances for bubble breakdown. As the concentration of nanoparticles grows, so does the value of the heat transfer coefficient. According to the findings, the optimal value for enhancement at high Reh is 2 g/L, whereas at low Reh, the value is 1 g/L. As the concentration increases, the heat transfer coefficient drops down somewhat. There seems to be no observable pattern of improvement with increasing N. By enhancing the thermal conductivity of gas-liquid dispersion under turbulent circumstances, when the influence of tiny bubbles is diminished, a 135% increase in heat transfer is obtained. Adding nanoparticles forces the Uo-reducing tiny bubbles to merge into bigger ones. Nanoparticles distort tiny bubbles into bigger ones, and their collisions create turbulent intensities that destroy the thermal boundary layer. In the presence of gas dispersion and nanofluids, friction is reduced because viscosity is decreased by the effect of increased mobility [Brodkey and Hershey, 1998].

Symbol	**meaning**	**units**
U	Overall heat transfer coefficient	W/m2.K
Re	Reynolds number	
ΔT	Temperature difference	˚C
Q	Gas flow rate	m3/s
di	Impeller diameter	mm
d_pBubbles diameter mm		
N	Agitation speed	rpm
AS	Surface area	m2
Stdev	Standard deviation	
$\dot{n}$	Number of bubbles per second	
z	Degree of confidence level	
$\dot{Q}$	Heat transfer rate	W
Cp	Heat capacity	J/Kg. K
K	Thermal conductivity	W/m. K
*F*Friction factor		
ΔP	Pressure drop	Cm-H2O
L	Tube or shell length	m
V	Tank volume	L
C	Nanoparticles concentration	g/L
U∞	Liquid velocity	m/s

Greek letters

Symbol	**meaning**	**units**
μDynamic viscosity	Kg/m. s	
a	Interfacial area	m-1
ρ	Density	Kg/m3
α	Gas void fraction	

Subscribes

i	Impeller
b	bubbles
T	tank diameter
h	hot water
c	cold water
g	gas
o	outside surface of tube

References

[1] A. S. Kasumu, N. N. Nassar, and A. K. Mehrotra, “A heat-transfer laboratory experiment with shell-and-tube condenser,” *Educ. Chem. Eng.*, vol. 19, pp. 38–47, 2017, doi: 10.1016/j.ece.2017.03.002.

[2] M. Sheikholeslami, M. Hatami, M. Jafaryar, F. Farkhadnia, D. D. Ganji, and M. Gorji-Bandpy, “Thermal management of double-pipe air to water heat exchanger,” *Energy Build.*, vol. 88, pp. 361–366, 2015, doi: 10.1016/j.enbuild.2014.11.076.

[3] J. yong Kim and A. J. Ghajar, “A general heat transfer correlation for non-boiling gas-liquid flow with different flow patterns in horizontal pipes,” *Int. J. Multiph. Flow*, vol. 32, no. 4, pp. 447–465, 2006, doi: 10.1016/j.ijmultiphaseflow.2006.01.002.

[4] E. E. Michaelides, *Particles, bubbles & drops: their motion, heat and mass transfer*. London, 2006. doi: 10.1243/03093247V281031.

[5] W.-D. Deckwer, “On the mechanism of heat transfer in bubble column reactors,” *Chem. Eng. Sci.*, vol. 35, no. 6, pp. 1341–1346, 1979, doi: 10.1016/0009-2509(80)85127-X.

[6] J. B. Joshi, M. M. Sharma, Y. T. Shah, C. P. P. Singh, M. Ally, and G. E. Klinzing, “Heat transfer in multiphase contactors,” *Chem. Eng. Commun.*, vol. 6, no. 4–5, pp. 257–271, 1980, doi: 10.1080/00986448008912534.

[7] G. A. Hughmark, “Holdup and heat transfer in horizontal slug gas-liquid flow,” *Chem. Eng. Sci.*, vol. 20, no. 12, pp. 1007–1010, 1965, doi: 10.1016/0009-2509(65)80101-4.

[8] S. C. Saxena and N. S. Rao, “Heat transfer and gas holdup in a two-phase bubble column: Air-water system — Review and new data,” *Exp. Therm. Fluid Sci.*, vol. 4, no. 2, pp. 139–151, 1991, doi: 10.1016/0894-1777(91)90058-Y.

[9] F. P. A. B. P. A. B. Scargiali, “Gas-liquid dispersions in mechanically agitated contactors Head of PhD Board,” *Fac. di Ing. - Dip. di Ing. Chim. dei Process. e dei Mater. Dottorato di Ric. “Tecnologie Chim. e dei nuovi Mater. XVIII Ciclo Sett. Sci. Discip. ING-IND/25 Impianti Chim. Gas-liquid*, pp. 1999–16, 2000.

[10] M. S. Liu, M. C. C. Lin, and C. C. Wang, “Enhancements of thermal conductivities with cu, CuO, and carbon nanotube nanofluids and application of MWNT/water nanofluid on a water chiller system,” *Nanoscale Res. Lett.*, vol. 6, no. 1, pp. 1–13, 2011, doi: 10.1186/1556-276X-6-297.

[11] K. S. Borate, P. P. M. Khanwalkar, and P. V. N. Kapatkar, “Heat Transfer Enhancement with Different Square Jagged Twisted Tapes and CuO / water Nano fluid,” *Int. J. Innov. Stud. Sci. Eng. Technol.*, vol. 4863, no. February, pp. 2–6, 2016.

[12] V. N. Rao and B. R. Sankar, “CFD analysis of CuO / water nanofluid flow in a double pipe U-Bend heat exchanger,” *Int. J. Dyn. Fluid*, vol. 13, no. 1, pp. 137–152, 2017.

[13] T. Hayat and S. Nadeem, “Heat transfer enhancement with Ag–CuO/water hybrid nanofluid,” *Results Phys.*, vol. 7, pp. 2317–2324, 2017, doi: 10.1016/j.rinp.2017.06.034.

[14] L. S. Tong and Y. S. Tang, *Boiling heat Transfer and Two-Phase Flow*. 1997.

[15] D. Kim, A. J. Ghajar, R. L. Dougherty, and V. K. Ryali, “Comparison of 20 two-phase heat transfer correlations with seven sets of experimental data, including flow pattern and tube inclination effects,” *Heat Transf. Eng.*, vol. 20, no. 1, pp. 15–40, 1999, doi: 10.1080/014576399271691.

[16] Robert C. Hendricks and Robert R. Sharp Lewis, “INITIATION OF COOLING DUE TO BUBBLE GROWTH ON A HEATING SURFACE,” *Natl. Aeronaut. Sp. Adm.*, no. April 1964, pp. 1–9, 1964.

[17] B. A. Abid, Nada Mahdi Farhan, and Shurooq Talib Al-Hemeri, "EFFECT OF PHYSICAL PROPERTIES ON HEAT TRANSFER AND FLOW REGIMES IN BUBBLE COLUMNS," *Al-Qadisiyah J. Eng. Sci.*, vol. 8, no. 2, pp. 171–185, 2015, doi: 10.4271/2013-01-1601.

[18] H. S. Kim *et al.*, "Bubble and Heat Transfer Phenomena in Viscous Slurry Bubble Column," *Adv. Chem. Eng. Sci.*, vol. 04, no. 04, pp. 417–429, 2014, doi: 10.4236/aces.2014.44046.

[19] B. O. Hasan, "Experimental study on the bubble breakage in a stirred tank. Part 1. Mechanism and effect of operating parameters," *Int. J. Multiph. Flow*, 2017, doi: 10.1016/j.ijmultiphaseflow.2017.08.006.

[20] C. W. Stewart, "Bubble interaction in low-viscosity liquids," *Int. J. Multiph. Flow*, vol. 21, no. 6, pp. 1037–1046, 1995, doi: 10.1016/0301-9322(95)00030-2.

[21] J. Tzeng, R. C. Chen, and L. A. Fan, "Visualization of Flow Characteristics in a 2-D Bubble Column and Three-Phase Fluidized Bed," *AIChE J.*, vol. 39, no. 5, pp. 733–744, 1993.

[22] W. A. Al-masry and E. M. Ali, "Identification of hydrodynamics characteristics in bubble columns through analysis of acoustic sound measurements — Influence of the liquid phase properties," *Chem. Eng. Process.*, vol. 46, pp. 127–138, 2007, doi: 10.1016/j.cep.2006.05.008.

[23] B. O. Hasan, "Breakage of drops and bubbles in a stirred tank: A review of experimental studies," *Chinese J. Chem. Eng.*, vol. 25, no. 6, pp. 698–711, 2017, doi: 10.1016/j.cjche.2017.03.008.

[24] K. B. Rao and P. S. Murti, "Heat Transfer in Mechanically Agitated Gas-Liquid Systems," *Ind. Eng. Chem. Process Des. Dev.*, vol. 12, no. 2, pp. 190–197, 1973, doi: 10.1021/i260046a011.

[25] E. De Maerteleire, "Heat transfer to a helical cooling coil in mechanically agitated gas-liquid dispersions," *Chem. Eng. Sci.*, vol. 33, no. 8, pp. 1107–1113, 1978, doi: 10.1016/0009-2509(78)85016-7.

[26] O. N. Kashinsky, V. V. Randin, and A. V. Chinak, "Heat transfer and shear stress in a gas-liquid flow in an inclined flat channel," *J. Eng. Thermophys.*, vol. 23, no. 1, pp. 39–46, 2014, doi: 10.1134/S1810232814010056.

[27] H. S. Dizaji and S.Jafarmadar, "Heat transfer enhancement due to air bubble injection into a horizontal double pipe heat exchanger," *Int. J. Autom. Eng.*, vol. 4, no. 4, 2014.

[28] P. Vlasogiannis, G. Karagiannis, P. Argyropoulos, and V. Bontozoglou, "Air – water two-phase flow and heat transfer in a plate heat exchanger," *Multiph. Flow*, vol. 28, pp. 757–772, 2002.

[29] G. J. Xu, Y. M. Li, Z. Z. Hou, L. F. Feng, and K. Wang, "Gas-liquid Dispersion and Mixing Characteristics and Heat Transfer in a Stirred Vessel," *Can. J. Chem. Eng.*, vol. 75, pp. 2–9, 1997.

[30] A. Cioncolini and J. R. Thome, "Prediction of the entrained liquid fraction in vertical annular gas-liquid two-phase flow," *Int. J. Multiph. Flow*, vol. 36, no. 4, pp. 293–302, 2010, doi: 10.1016/j.ijmultiphaseflow.2009.11.011.

[31] L. E. Ortiz-Vidal, N. Mureithi, and O. M. H. Rodriguez, "Two-Phase Friction Factor in Gas-Liquid Pipe Flow," *Rev. Eng. Térmica*, vol. 13, no. 2, p. 81, 2014, doi: 10.5380/reterm.v13i2.62101.

[32] A. Zamzamian, S. N. Oskouie, A. Doosthoseini, A. Joneidi, and M. Pazouki, "Experimental investigation of forced convective heat transfer coefficient in nanofluids of Al2O3/EG and CuO/EG in a double pipe and plate heat exchangers under turbulent flow," *Exp. Therm. Fluid Sci.*, vol. 35, no. 3, pp. 495–502, 2011, doi: 10.1016/j.expthermflusci.2010.11.013.

[33] V. Bianco, O. Manca, S. Nardini, and K. Vafai, *Heat Transfer Enhancement with Nanofluids*. New York: CRC Press, 2015. [Online]. Available: https://books.google.com.my/books?id=v5S9BwAAQBAJ

[34] O. K. Hamilton, R. L., and Crosser, "Thermal conductivity of heterogeneous two-component system.," *Ind. Eng. Chem. Fundam.*, vol. 1, no. 3, pp. 187–191, 1962.

[35] M. Corcione, "Rayleigh-Bénard convection heat transfer in nanoparticle suspensions," *Int. J. Heat Fluid Flow*, 2011, doi: 10.1016/j.ijheatfluidflow.2010.08.004.

[36] W. Duangthongsuk and S. Wongwises, "Heat transfer enhancement and pressure drop characteristics of TiO2-water nanofluid in a double-tube counter flow heat exchanger," *Int. J. Heat Mass Transf.*, vol. 52, no. 7–8, pp. 2059–2067, 2009, doi: 10.1016/j.ijheatmasstransfer.2008.10.023.

[37] A. A. R. Darzi, M. Farhadi, and K. Sedighi, "Heat transfer and flow characteristics of AL2O3-water nanofluid in a double tube heat exchanger," *Int. Commun. Heat Mass Transf.*, vol. 47, pp. 105–112, 2013, doi: 10.1016/j.icheatmasstransfer.2013.06.003.

[38] R. Aghayari, H. Maddah, M. Zarei, M. Dehghani, and S. G. Kaskari Mahalle, "Heat Transfer of Nanofluid in a Double Pipe Heat Exchanger," *Int. Sch. Res. Not.*, vol. 2014, pp. 1–7, 2014, doi: 10.1155/2014/736424.

[39] J. Albadr, S. Tayal, and M. Alasadi, "Heat transfer through heat exchanger using Al2O3nanofluid at different concentrations," *Case Stud. Therm. Eng.*, vol. 1, no. 1, pp. 38–44, 2013, doi: 10.1016/j.csite.2013.08.004.

[40] A. Rostamzadeh, K. Jafarpur, E. Goshtasbirad, and M. M. Doroodmand, "Experimental investigation of mixed convection heat transfer in vertical tubes by nanofluid: Effects of reynolds number and fluid temperature," *Int. J. Eng. Trans. B Appl.*, vol. 27, no. 8, pp. 1251–1258, 2014, doi: 10.5829/idosi.ije.2014.27.08b.11.